INDERSCIENCE PUBLISHERS
Linking academia, business and industry through research

International Journal of Surface Science and Engineering

ISSN online: 1749-7868 - ISSN print: 1749-785X
https://www.inderscience.com/ijsurfse

Non-contact surface roughness measurement of blasted specimens using machine vision technique

Kyungmok Kim

DOI: 10.1504/IJSURFSE.2024.10065742

Article History:

Received:	23 February 2024
Last revised:	01 May 2024
Accepted:	18 May 2024
Published online:	04 March 2025

Non-contact surface roughness measurement of blasted specimens using machine vision technique

Kyungmok Kim

School of Aerospace and Mechanical Engineering,
Korea Aerospace University,
76 Hanggongdaehak-ro, Deogyang-gu,
Goyang-si, Gyeongi-do, 412-791, South Korea
Email: kkim@kau.ac.kr

Abstract: This article describes non-contact surface roughness measurement for shot and grit blasted specimens. A simple machine vision algorithm was proposed for determining ten-point mean roughness (R_z) of a specimen after shot and grit blasting. Surfaces cleaned with different blast abrasives were captured by a microscope. Binary images were then created by using Otsu's thresholding method. On the binary image, bright regions were selected, associated with specular reflection of light. The average size of selected regions was calculated in this proposed method. It was found that the average size has a linear relation with ten-point mean roughness of both shot and grit blasted surfaces. It was also identified that the parameter of a linear regression for shot blasting is different from that for grit blasting. On the basis of the relation, it is possible to determine the ten-point mean roughness of a blasted surface with a captured surface image.

Keywords: shot blasting; grit blasting; machine vision; surface roughness.

Reference to this paper should be made as follows: Kim, K. (2025) 'Non-contact surface roughness measurement of blasted specimens using machine vision technique', *Int. J. Surface Science and Engineering*, Vol. 19, No. 1, pp.61–75.

Biographical notes: Kyungmok Kim received his PhD in Oxford University, UK. He is a Professor in the School of Aerospace and Mechanical Engineering of Korea Aerospace University. His fields of expertise are tribology and contact mechanics.

1 Introduction

Abrasive blasting is a well-known surface pre-treatment process in surface engineering (Efremov and Gerasimova, 2021). Abrasive media such as steel shots and grits lead to localised plastic deformation by hitting a target surface at high velocity. Shot blasting typically uses a spherical steel shot which creates a smooth texture on a target surface. Grit blasting uses a metallic grit which is randomly angular. Grit blasting produces a controlled surface with low effort and easily implemented in industrial applications (Yetik et al., 2020).

Roughness of the blasted surface is dependent upon abrasive medium size. In order to obtain low surface roughness, fine shots or grits are selected during a blasting process. In

a manufacturing industry, surface roughness after abrasive blasting is often measured with manual comparison (e.g., tactile or visual perception with a sample comparator) (ASTM D4417, 2021) or with a measuring instrument such as a contact-based profilometer and a non-contact laser scanner (Bhushan, 2002; Kim and Baek, 2023; Santhanakrishnan et al., 2024). Manual comparison is preferred in industry in terms of cost and convenience. However, human errors exist, thereby decreasing the measurement accuracy of surface roughness. A contact-based profilometer (e.g., stylus profilometer) and a laser scanner enable measuring surface roughness with low measuring errors. However, measurement range and working environment are limited. Particularly, a laser scanning method for surface roughness is rather expensive. Thus, these methods are more preferred in a research lab than an industrial field.

Machine vision technique has come to be remarkable in the measurement of surface roughness, since computing power has increased rapidly. Various machine vision and machine learning techniques are being developed to overcome the disadvantages of the conventional measurement methods described above (Tsai et al., 1998; Al-Kindi and Shirinzadeh, 2007; Lee et al., 2005; Kumar et al., 2005; Giusti et al., 2020; Cerro et al., 2021; Kumar and Jain, 2022; Yang et al., 2022; Kim, 2022; Basyoni et al., 2023; Yan et al., 2022). A machine vision system was proposed to assess the surface roughness of machined parts produced by shaping and milling processes (Tsai et al., 1998). A neural network algorithm was developed for roughness assessment of shaped and milled surfaces. Surface roughness measurement using vision-based data was proposed and roughness parameters were evaluated (Al-Kindi and Shirinzadeh, 2007). Vision data was interpreted with a light reflection model, called the intensity-topography compatible model. Various roughness parameters such as R_q, R_t and R_p were compared with those measured with a stylus profilometer. An adaptive neuro-fuzzy inference system was developed for estimation of surface roughness from texture features in turning operations (Lee et al., 2005). The neuro-fuzzy inference system was used for establishing the relationship between the arithmetic average surface roughness (R_a) and texture feature of a captured surface image. A cubic convolution interpolation technique was proposed for magnifying and analysing surface images (Kumar et al., 2005). Correlation between magnification index and roughness was established for ground, milled, and shaped surfaces. Image-based surface roughness measurement was proposed using machine learning (Giusti et al., 2020). Convolutional neural network (CNN) was used to evaluate Ra on a small image of workpiece-surfaces machined by die-sinking EDM. A machine learning algorithm based on a multilayer perception was employed to generate models and predict R_a of 3D printed parts (Cerro et al., 2021). An attempt to predict surface roughness was carried out with K-nearest neighbours (KNN) algorithm (Kumar and Jain, 2022). KNN algorithm was used for predicting R_a of the surface generated with micro-plasma transferred arc metal additive manufacturing process. A recent study proposed anti-interference roughness detection method based on image inpainting and CNN algorithm (Yang et al., 2022). The CNN model, CBAM Res-Unet model, and PConv-Net model were combined in a complete anti-interference detection method for machined surfaces containing chips. Texture recognition method was introduced with an arc-shaped soft tactile sensor and a bidirectional long short-term memory model (Yan et al., 2022). Deep leaning-enhanced tactile sensing technique was developed for real-time recognition of surface texture. Computer vision technique was proposed for anti-fretting coatings (Kim, 2022). In the study, fretting wear damage on coated systems was identified with computer vision technique. The technique was merely useful for worn surfaces of a solid

coating. Machine learning approach was proposed for surface roughness quantification (Basyoni et al., 2023). Two-point correlation function and lineal-lath function were used to quantify surface roughness of battery materials.

Despite a variety of studies have been carried out on predicting surface roughness, little is found on research associated with roughness prediction of a blasted surface. In this study, a simple and fast machine vision method is proposed for determining the surface roughness of shot-and grit-blasted specimens. In order to overcome disadvantages of conventional measurement techniques, surface images captured with a microscope were used in the proposed method. Surface images were analysed with the algorithm written in MATLAB. Regions of specular reflection locally distributed on a blasted surface were identified, and then the average size of the selected regions was calculated. Finally, correlation between the average size and ten-point mean roughness (R_z) of a blasted specimen was identified.

2 Experimental setup

Figure 1 shows the proposed machine vision system. A microscope with light sources was used for capturing surface images. The vertical distance between the microscope and a target surface was set to 5 cm. A captured surface image was transferred to a workstation that the machine vision algorithm was installed on. The developed algorithm code was written in MATLAB. Detail of codes is shown in the Appendix. Ten-point mean roughness (Rz) of the captured surface was printed as a result of image analysis.

Figure 1 Schematic diagram of a machine vision system (see online version for colours)

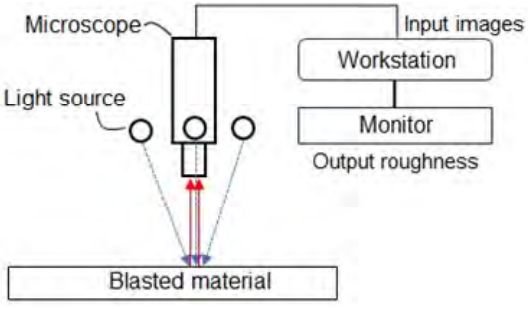

In this study, blast-cleaned surfaces were prepared with shot and grit abrasives (supplier: Paint Test equipment Inc. USA); Continuous impact of the abrasive with a diameter of greater than 0.4 mm (high carbon cast steel of 53-60 HRC) was applied on to the target surface at high speed of 65-110 m/s. All mill-scale rust and foreign particles were removed via a jet stream of compressed air. And then, the surface was cleaned with dry compressed air, according to standardised preparation grades (blast cleaning of Sa 3). The ten-point mean roughness (R_z) values of three shot-blasted surfaces were 40 ± 5 µm, 70 ± 10 µm and 100 ± 15 µm, respectively. R_z values of three grit-blasted surfaces were 60 ± 10 µm, 100 ± 15 µm, and 150 ± 20 µm, respectively. In this study, four surface images were captured at random locations on the surface.

3 Results and discussion

An overall procedure from image input to roughness output is described in Figure 2. A greyscale image is used for this algorithm. If an RGB format image is submitted to the algorithm, it is necessary to convert RGB to grayscale format. In this study, Otsu's method is used, one of well-known techniques for image thresholding (Otsu, 1979). The method enables separating a submitted image into two classes: foreground and background. The foreground corresponds to the region of specular reflection, whereas background is associated to the region of scattered reflection. An optimal threshold value detected on the greyscale histogram of the image is permitted to separation of two regions.

Figure 2 The proposed method for calculation of surface roughness (see online version for colours)

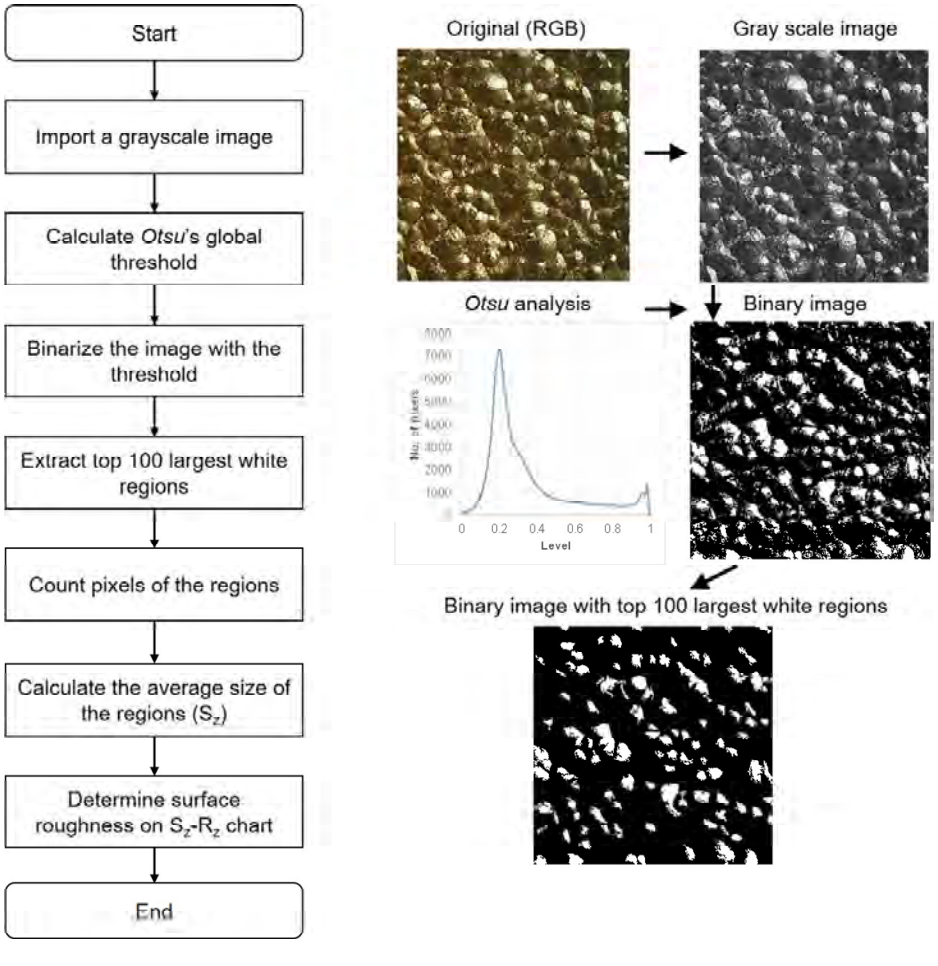

Figure 3 Images for shot blasted specimens with R_z of 40 µm, (a, d, g, j) greyscale (b, e, h, k) binary images (c, f, i, l) those with top 100 largest white regions

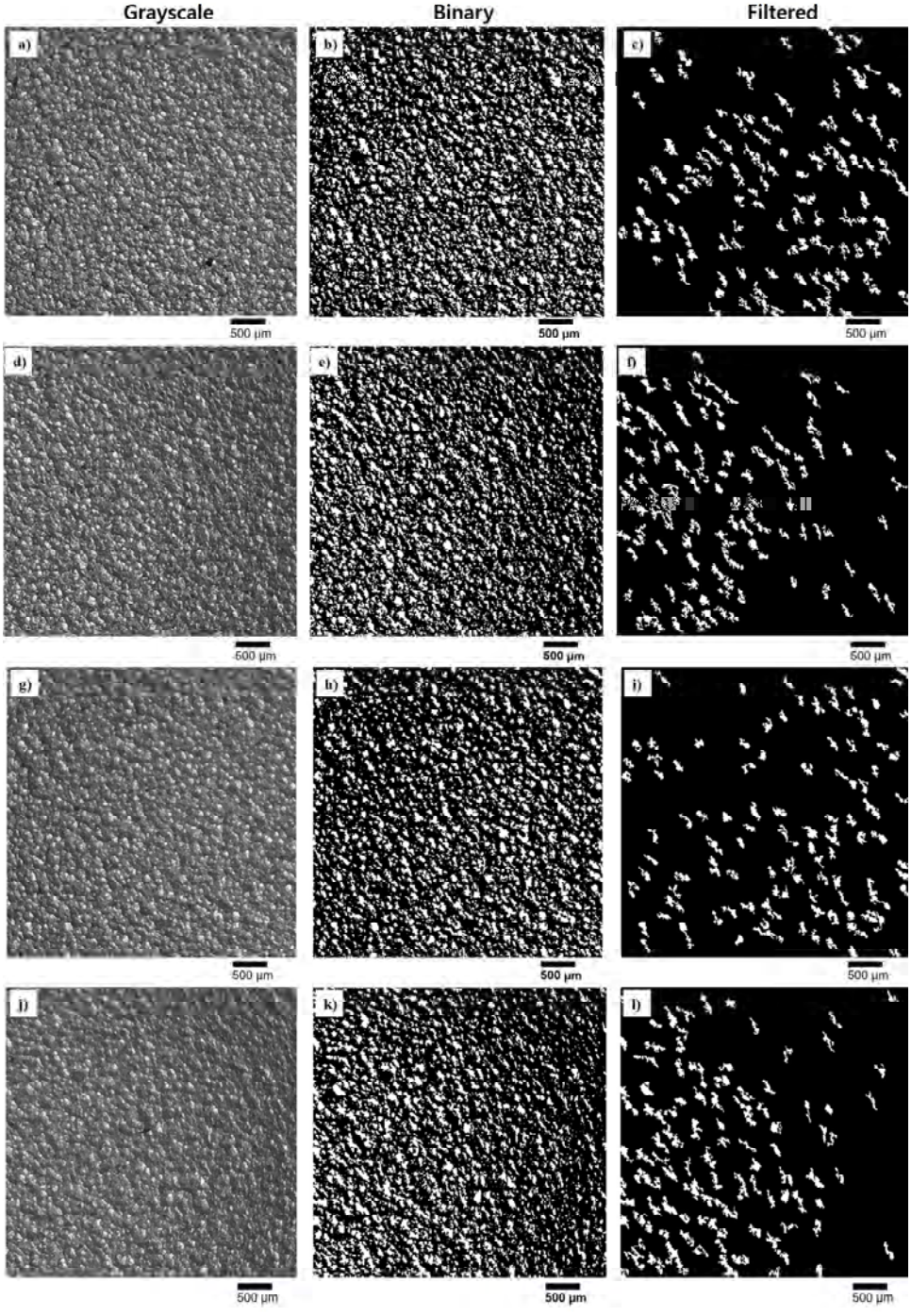

Figure 4 Images for shot blasted specimens with R_z of 70 µm, (a, d, g, j) greyscale (b, e, h, k) binary images (c, f, i, l) those with top 100 largest white regions

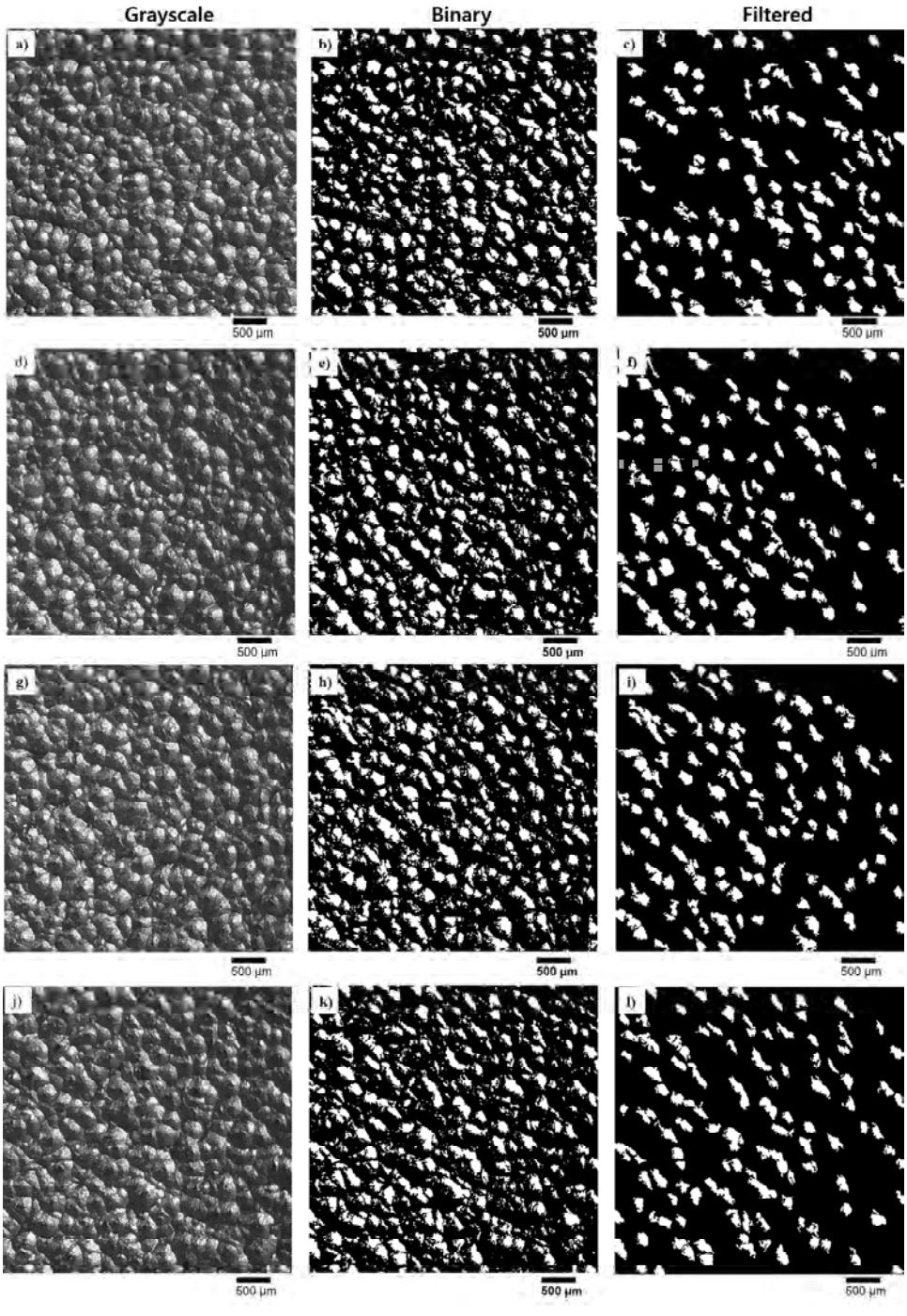

Figure 5 Images for shot blasted specimens with R_z of 100 µm, (a, d, g, j) greyscale (b, e, h, k) binary images (c, f, i, l) those with top 100 largest white regions

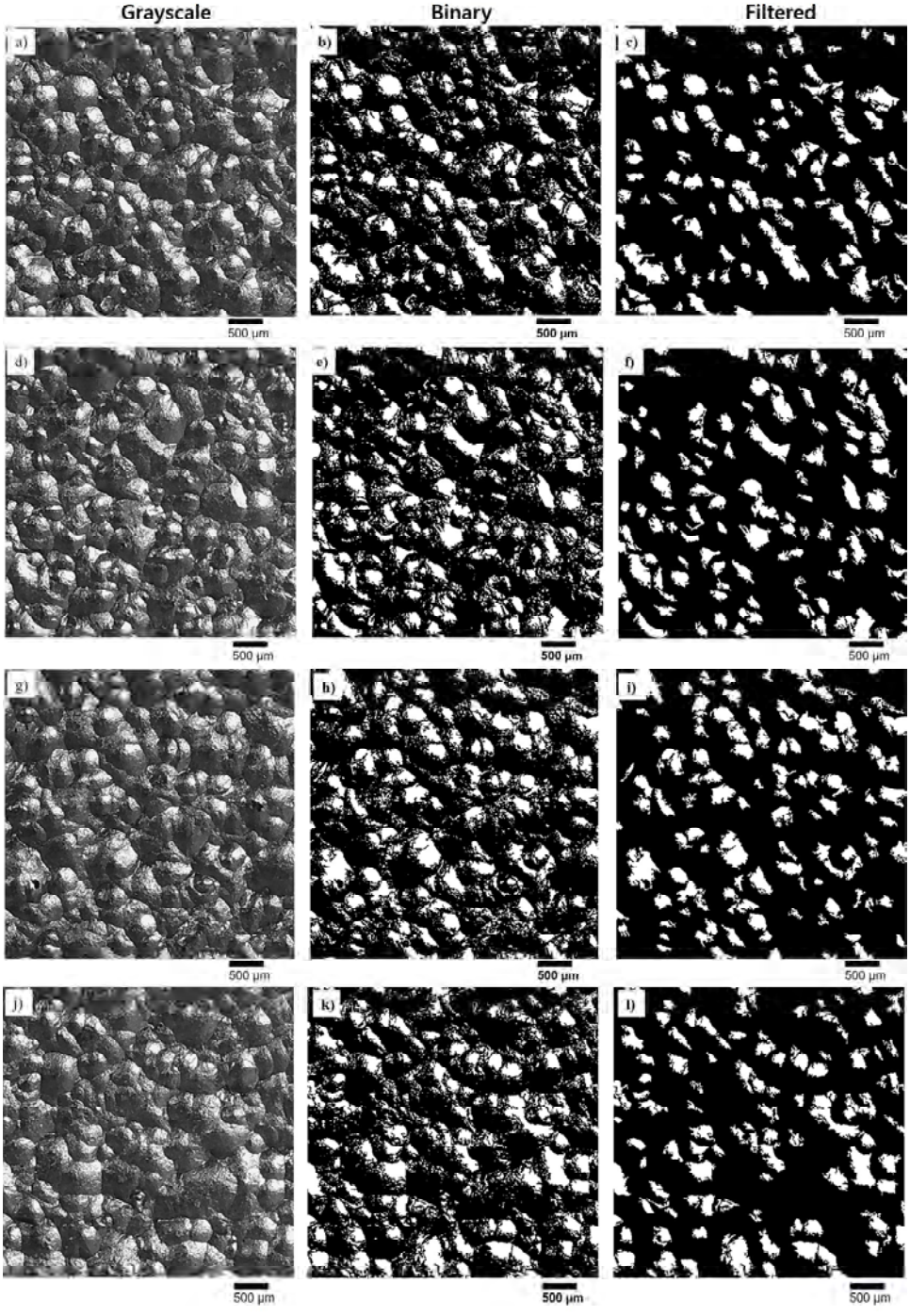

Figure 6 Images for grit blasted specimens with R_z of 60 µm, (a, d, g, j) greyscale (b, e, h, k) binary images (c, f, i, l) those with top 100 largest white regions

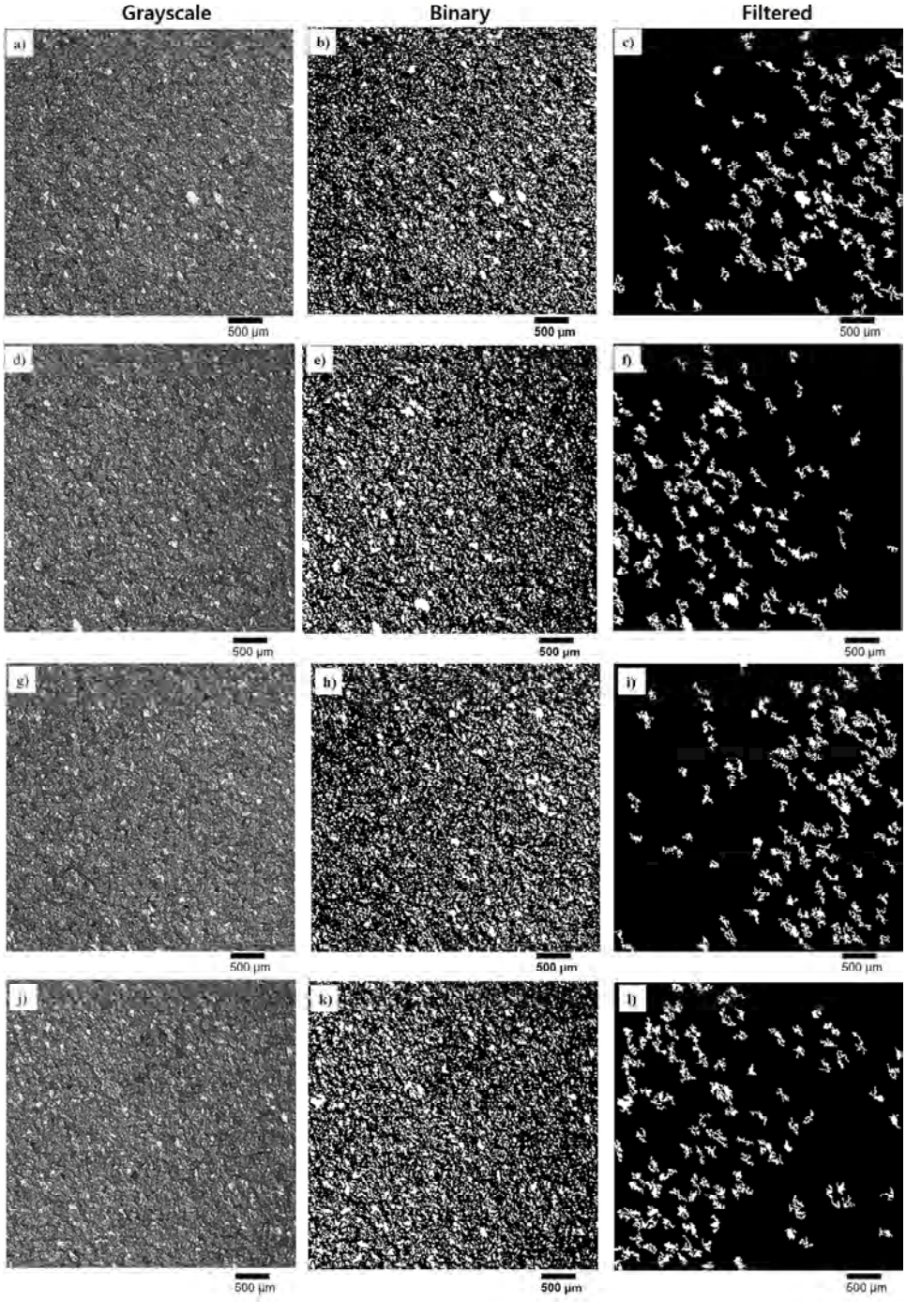

Figure 7 Images for grit blasted specimens with R_z of 100 µm, (a, d, g, j) grayscale (b, e, h, k) binary images (c, f, i, l) those with top 100 largest white regions

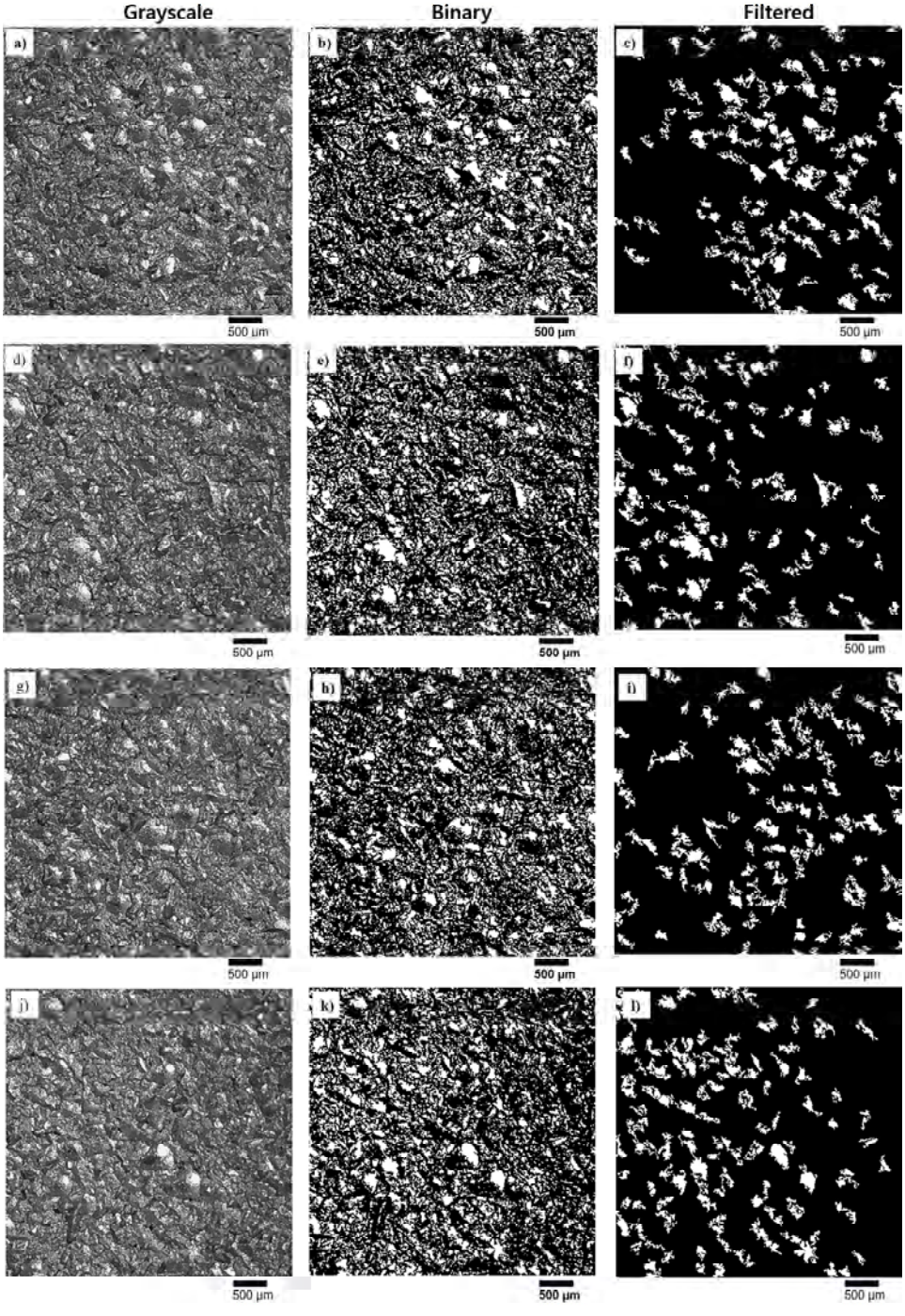

Figure 8 Images for grit blasted specimens with R_z of 150 µm, (a, d, g, j) greyscale (b, e, h, k) binary images (c, f, i, l) those with top 100 largest white regions

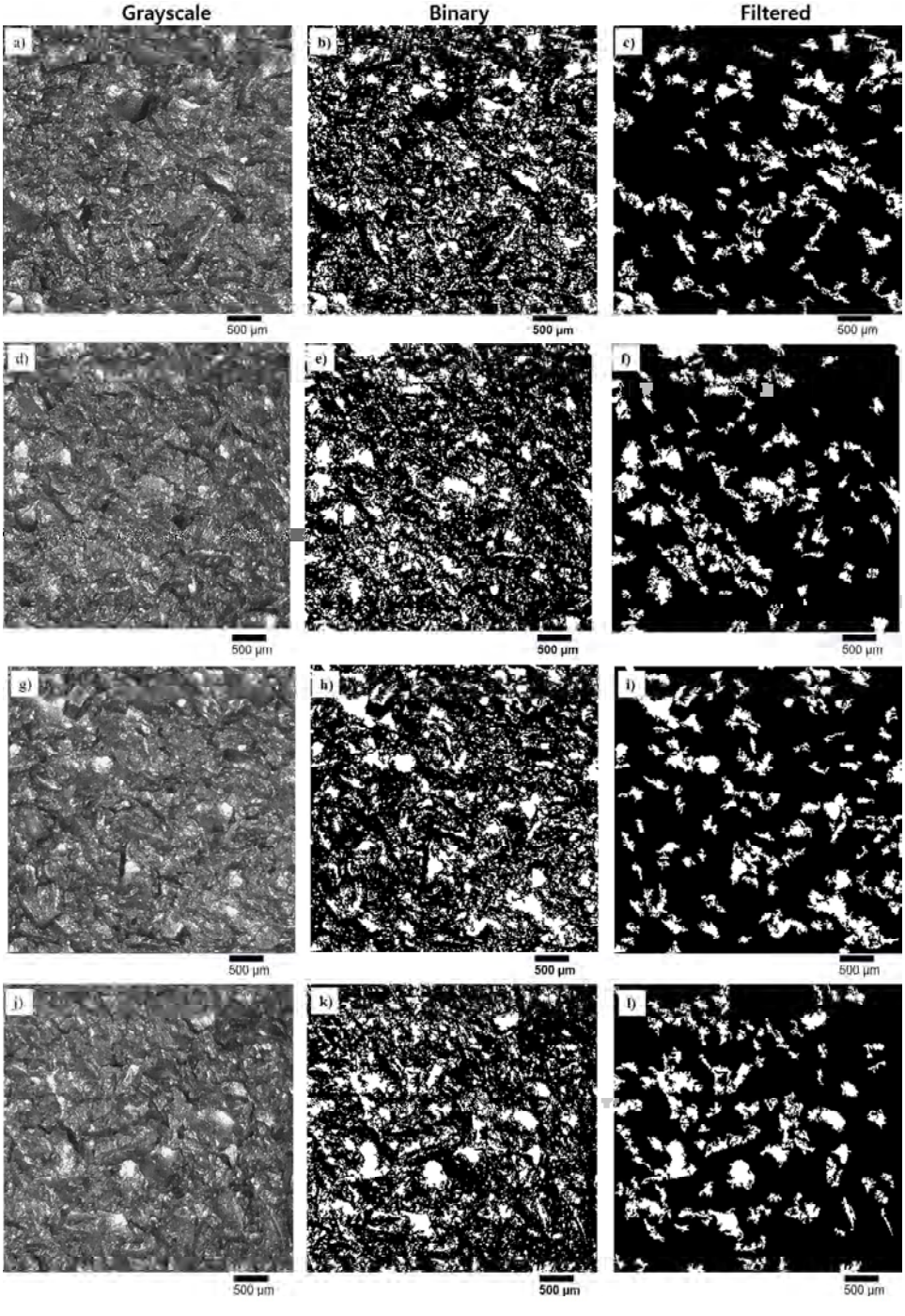

The image is then binarised with the calculated threshold. On the binary image, white regions resulted from specular reflection of light. In this study, it was assumed that the size of a white region is associated with the magnitude of roughness. Thus, white regions of the image are selected and then pixels of the selected regions are counted; one hundred largest regions were chosen in this algorithm. The number of pixels counted (n_c) is used for determining the average size of the white regions. That is, the average size (S_z) is defined as

$$S_z = \frac{n_c}{n_s} \tag{1}$$

where n_s denotes the number of selected regions (here, it corresponds to a value of 100).

Finally, surface roughness can be determined on the correlation between ten-point mean roughness and the average size. Correlation between ten-point mean roughness and the average size needs to be predetermined with shot-and grit-blasted specimen. The correlation could be obtained by using a sample comparator for which the roughness is known.

Table 1 Otsu's thresholds determined automatically

Figure no.	*Type of abrasive*	*R_z [µm]*	*Otsu's threshold*			
			Image a	*Image d*	*Image g*	*Image j*
3	Shot	40	0.4941	0.4784	0.4863	0.4706
4		70	0.4902	0.4824	0.4980	0.4706
5		100	0.5059	0.5098	0.4902	0.5059
6	Grit	60	0.4549	0.4549	0.4706	0.4667
7		100	0.4784	0.4824	0.4667	0.4902
8		150	0.4745	0.4784	0.4980	0.4784

Table 2 The average size of top 100 white regions (S_z)

Figure no.	*Type of abrasive*	*R_z [µm]*	*S_z (No. of pixels)*				*Average number of pixels*
			Image a	*Image d*	*Image g*	*Image j*	
3	Shot	40	296	272	265	286	279.8
4		70	513	478	525	498	503.5
5		100	589	630	661	655	633.8
6	Grit	60	283	268	267	288	276.5
7		100	424	384	420	454	420.5
8		150	473	494	563	531	515.3

Note: Total number of pixels of each image was 360,000.

Figures 3(a), 3(d), 3(g) and 3(j) shows grayscale images of shot-blasted specimens with Rz of 40 µm. Bright parts are associated with specular reflection of light. The figures were converted into a binary format as shown in Figures 3(b), 3(e), 3(h) and 3(k). To generate the binary image, Otsu's method was applied to a greyscale image. Table 1 shows Otsu's thresholds calculated automatically for each image. On the binary image, the top 100 largest white regions were selected and presented on Figures 3(c), 3(f), 3(i)

and 3(l). Figures 4 and 5 show the images for shot-blasted surfaces with R_z of 70 µm and 100 µm, respectively. It was identified that each white regions tended to enlarge with increased roughness parameter, R_z. Binary images containing the top 100 largest white regions were presented as Figures 4(c), 4(f), 4(i) and 4(l) for R_z of 70 µm, and as Figures 5(c), 5(f), 5(i) and 5(l) for R_z of 100 µm. Figures 6, 7, and 8 show the images for grit blasted surfaces with R_z of 60 µm, 100 µm, and 150 µm, respectively. Surfaces of the binary images for R_z of 100 µm in Figures 7(b), 7(e), 7(h) and 7(k) were different from those found for shot-blasted surfaces in Figures 5(b), 5(e), 5(h) and 5(k); white parts of grit blasted surfaces were irregular and angular, whereas those of shot blasted surfaces were close to spherical. In addition, the size of the part on a grit blasted surface was smaller than the size found on a shot blasted surface, under the condition of the same abrasive medium size. It was found from Figures 6, 7 and 8 that top 100 largest white regions tended to enlarge according to increase of grit size. In order to find out the relationship between the region size and the ten-point mean roughness (R_z), the size of the selected white regions was calculated by counting the number of white pixels. Then, the average size of the selected regions was determined. Table 2 shows the average size of top 100 white regions in terms of number of pixels.

Figure 9 Correlation between the average size of specular reflection regions (S_z) and ten-point mean roughness (R_z)

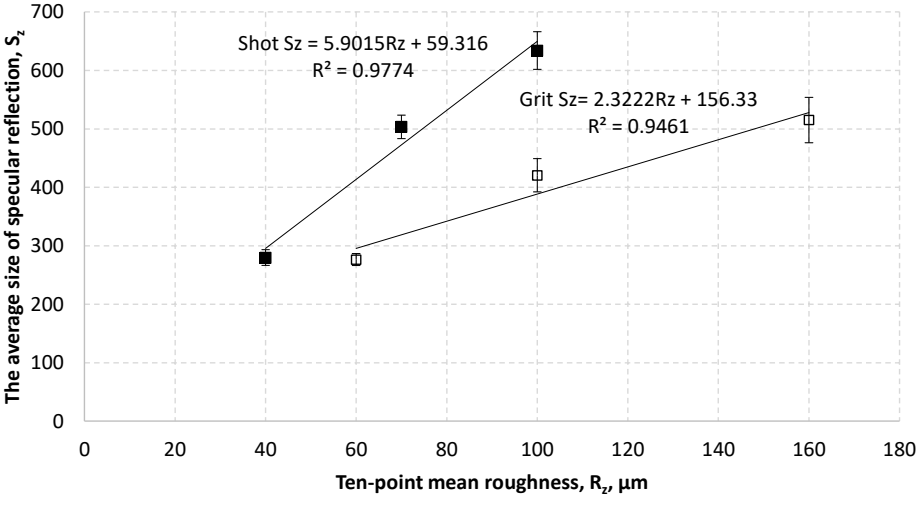

Note: Error bars represent 95% confidence intervals.

Figure 9 shows the average size (S_z) according to ten-point mean roughness (R_z) of the blasted surfaces. Four captured images were used for calculating the average size at each roughness level. It was identified that a linear relation between S_z and R_z was found on both shot- and grit-blasted surfaces. In addition, the increase rate of the average size for shot-blasting was greater than that for grit-blasting. On the figure, R-squared presents that a good linear regression was obtained. The error bar represents 95% confidence intervals. The relationship between S_z and R_z could be used for predicting the ten-point mean roughness of shot or grit blasted surfaces with a captured surface image within chosen roughness ranges. In other words, the ten-point mean roughness can be expressed as a function of the average size of specular reflection, identified via a captured surface

image. In this study, a captured image was 4.2 x 4.2 mm in size (600 x 600 pixels). With this image size, it is difficult to identify waviness, one of important characteristics in surface texture. Thus, a method to determine waviness on captured images will be needed.

The linear relation on Figure 9 is empirical and valid only within the chosen roughness range. Note that, in this study, surface roughness ranged from 40 μm to 100 μm for shot blasting, and from 60 μm to 150 μm for grit blasting. Therefore, a theoretical model needs to be established, describing the relation between the average size of specular reflection and ten-point mean roughness. In this research, ten-point mean roughness was merely used. Thus, additional studies on a correlation between the average size of specular reflection and another roughness parameter would be interesting, and remain as future work.

4 Conclusions

In this study, non-contact surface roughness measurement was described for shot-and grit-blasting cleaned surfaces. A simple algorithm to determine ten-point mean roughness on a captured blasted image was proposed. In the machine vision algorithm, a grayscale image was used and then converted into a binary format by using Otsu's method. Bright regions corresponding to specular reflection of light were identified on surface images prepared with various roughness values. The top 100 largest regions were then extracted from each surface image. The average size of selected regions was computed.

It was found that the average size of the regions tends to increase with increased ten-point mean roughness on a blasted surface. That is, the correlation between the average size of the selected regions and ten-point mean roughness was found to be linear. A parameter in the form of a linear regression was observed to be different between shot-blasted and grit-blasted specimens; The increase rate of the average size in specular reflection for shot-blasting was greater than the increase rate for grit-blasting. Note that this form of the linear regression allows determining ten-point mean roughness of blasted surfaces with an image captured by a microscope. This proposed non-contact roughness measurement is fast and convenient; thus, it would be possible to measure surface roughness of a blasted specimen in a manufacturing process.

The obtained linear relation is empirical and valid only within the chosen roughness range. Therefore, a theoretical model needs to be established, describing the relation between the average size of specular reflection and ten-point mean roughness. In this study, four captured images of 4.2 × 4.2 mm in size were obtained at different locations of the blasted specimens. The average of S_z values was used. With the images, it is difficult to identify waviness, one of important characteristics in surface texture. Thus, additional method for determining waviness on captured images needs to be developed. In this study, ten-point mean roughness ranges of tested specimens were from 40 μm to 100 μm for shot blasting, and from 60 μm to 150 μm for grit blasting. Therefore, further work needs to investigate the relation between the average size and ten-point mean roughness at lower roughness levels. In addition, application to shot peened surfaces with various shot sizes would be of interest to the manufacturing sector. Other roughness parameters such as the arithmetic average roughness need to be taken into account in future work.

Acknowledgements

This work was supported by the National Research Foundation of Korea(NRF) grant funded by the Korea government(MSIT) (No. NRF-2022R1H1A2006352)

References

Al-Kindi, G.A. and Shirinzadeh, B. (2007) 'An evaluation of surface roughness parameters measurement using vision-based data', *International Journal of Machine Tools and Manufacture*, Vol. 47, Nos. 3–4, pp.697–708.

ASTM D4417 (2021) *Standard Test Methods for Field Measurement of Surface Profile of Blast Cleaned Steel*, ASTM International, West Conshohocken, PA, DOI: 10.1520/D4417-21.

Basyoni, M., Jiao, Y. and Allam, N.K. (2023) 'A novel machine learning approach for surface roughness quantification and optimization of cast-on-strap lead-antimony alloy via two-point correlation function', *Scientific Reports*, Vol. 13, No. 1, Article No. 13369, pp.1–11, https://doi.org/10.1038/s41598-023-39619-z.

Bhushan, B. (2002) *Introduction to Tribology*, pp.55–84, John Wiley & Sons, Hoboken, NJ, USA.

Cerro, A., Romero, P., Yigit, O. and Bustillo, A. (2021) 'Use of machine learning algorithms for surface roughness prediction of printed parts in polyvinyl butyral via fused deposition modelling', *The International Journal of Advanced Manufacturing Technology*, Vol. 115, No. 1, pp.2465–2475.1

Efremov, D. and Gerasimova, A. (2021) 'Shotblasting process for surface hardening', *Materials Today: Proceedings*, Vol. 38, No. 4, pp.1685–1688.

Giusti, A., Dotta, M., Maradia, U., Boccadoro, M., Gambardella, L.M. and Nasciuti, A. (2020) 'Image-based measurement of material roughness using machine learning techniques', *20th CIRP Conference on Electro Physical and Chemical Machine*, Vol. 95, No. 1, pp.377–382.

Kim, K. (2022) 'Evaluation of fretting wear damage on coated system using computer vision technique', *International Journal of Surface Science and Engineering*, Vol. 16, No. 2, pp.150–162.

Kim, K. and Baek, S.Y. (2023) 'Influence of counterpart materials on fretting wear of FDM printed polyactic acid plates', *International Journal of Precision Engineering and Manufacturing*, Vol. 24, No. 1, pp.1855–1863.

Kumar P. and Jain. N.K. (2022) 'Surface roughness prediction in micro-plasma transferred arc metal additive manufacturing process using K-nearest neighbors algorithm', *The International Journal of Advanced Manufacturing Technology*, Vol. 119, No. 1, pp.2985–2997.

Kumar, R., Kulashekar, P., Dhanasekar, B. and Ramamoorthy, B. (2005) 'Application of digital image magnification for surface roughness evaluation using machine vision', *International Journal of Machine Tools and Manufacture*, Vol. 45, No. 2, pp.228–234.

Lee, K.C., Ho, S.J. and Ho, S.Y. (2005) 'Accurate estimation of surface roughness from texture features of the surface image using an adaptive neuro-fuzzy inference system', *Precision Engineering*, Vol. 29, No. 1, pp.95–100.

Otsu, N. (1979) 'A threshold selection method from gray level histograms', *IEEE Transactions on Systems, Man and Cybernetics*, Vol. 9, No. 1, pp.62–66.

Santhanakrishnan, R., Varghese, A.J. and Kamaraj, M. (2024) 'Tribological characteristics of carbon fibre reinforced epoxy composite filled with ceramic particles: influence of multi-walled carbon nanotubes', *International Journal of Surface Science and Engineering*, Vol. 18, No. 1, pp.71–88.

Tsai, D.M., Chen, J.J. and Chen, J.F. (1998) 'A vision system for surface roughness assessment using neural networks', *International Journal of Advanced Manufacturing Technology*, Vol. 14, No. 1, pp.412–422.

Yan, Y., Hu, Z., Shen, Y. and Pan, J. (2022) 'Surface texture recognition by deep leaning-enhanced tactile sensing', *Advanced Intelligent Systems*, Vol. 4, No. 1, Article No. 2100076, pp.1–7, https://doi.org/10.1002/aisy.202100076.

Yang, J., Zou, B., Guo, G., Chen, W., Wang, X. and Zhang, K. (2022) 'A study on the roughness detection for machine surface covered chips based on deep learning', *Journal of Manufacturing Processes*, Vol. 84, No. 1, pp.77–87.

Yetik, O., Koçoğlu, H., Avcu, Y.Y., Avcu, E. and Sınmazçelik, T. (2020) 'The effects of grit size and blasting pressure on the surface properties of grit blasted Ti6Al4V alloy', *Materials Today: Proceedings*, Vol. 32, No. 1, pp.27–36.

Nomenclature

n_c Number of pixels counted.

n_s Number of selected regions.

S_z Average size of white regions.

R_z Ten-point mean roughness.

Appendix

Brief algorithm code written in MATLAB

```
Image_gray = rgb2gray(image_RGB);          % if an imported image is RGB format
level = graythresh(Image_gray);            % Otsu's threshold
BI = imbinarize(Image_gray, level);        % binary image generation with Otsu's threshold
Filtered_image = bwareafilt(BI, 100);      % selection of top 100 largest white regions
Ncount=0;
for i = 1:1:width                          % width of the image (no. of pixels)
    for j = 1:1:height                     % height of the image (no. of pixels)
        if Filtered_image (i, j) > 0.5     % unity corresponds to white
            Ncount = Ncount + 1;
        end
    end
end
```